The Korean Communications
in Statistics Vol. 4, No. 3, 1997
pp. 817 - 825

An Edge-detecting Bayesian Image Reconstruction for Positron Emission Tomography

Jongseok Um and Byongsu Choi[1)]

Abstract

Images reconstructed with EM algorithm have been observed to have checkerboard effects and have large distortions near edges as iterations proceed. We suggest a simple algorithm of applying line process to the EM and Bayesian EM to reduce the distortions near edges. We show by simulation that this algorithm improves the clarity of the reconstructed image and has good properties based on root mean square error.

1. Introduction

Positron emission tomography (PET) is a radiological technique to image the biological function of tissue in the organ. A subject is injected with a quantity of a positron emitting radioisotope. When the isotope decays, a pair of photons is emitted along a straight line from the anihilation site in the opposite directions. The direction of the line of flight is random in the space. Emitted photons are counted by a machine consisting of detectors. A pair of detectors which detect a pair of emitted photons is called detector tube. Let $f(x)$ be the intensity of the image at the point x and $g(y)$ be the recorded intensity at the detector tube y. Then we have the relationship between f and g by an operator R with $g = Rf$. The reconstruction problem is to estimate f given the data g. This is a mathematical inversion problem of solving equation $g = Rf$ for f when g is given and R is known. The operator R is linear and this problem is called linear inverse problem with positive constraints. In transformation method, R is a line integral Radon transformation and f is obtained from the inverse Radon transformation(Herman, 1980).

Alternatively, first dicretize the domain of f and g and then estimate f according to optimization criteria, which is called series expansion methods. In this discretizing setting, the data consist of a vector of counts detected in the dth detector tube $n^*(d)$, $d=1,2,\cdots,D$,

1) Assistant Professor, Department of Statistics, Hansung University, Seoul, 136-792, Korea.

where D is the total number of detector tubes. Let $\lambda(b)$ be the emission intensity at a point b in the image, $b=1,2,\cdots, B$, where B is the number of boxes in the image. Usually we choose a box as a pixel in the image. Assuming $n^*(d)$ as Poisson distribution with parameter $\lambda^*(d)$, optimization criteria is to maximize likelihod function. Let $n(b,d)$ be the random variable denoting the number of radioactive emissions occuring in the pixel b and detected at the tube d. Regarding $n(b,d)$ as unobserved data and $n^*(d)$ as observed data, EM algorithm is applicable to find $\lambda(b)$, $b=1,2,\cdots, B$, which maximize likelihood function $p(\vec{n^*}|\vec{\lambda})$ (Vardi, shepp and Kaufman, 1985). However, EM algorithm have been observed to become noisy and have large distortions near edges as the algorithm converges toward the maximum likelihood estimates. Introducing a priori probability, maximum a posteriori image reconstruction using EM algorithm, Bayesian EM(BEM), prevents the occurrence of checkerboard effects in the image.

In this paper, we suggest a simple algorithm of applying line process to the EM and BEM to reduce the distortions near edges. We show by simulation that this algorithm improves the clarity of the reconstructed image and has good properties based on root mean square error(RMS).

2. Modeling for the PET

2.1 Likelihood for the emission counts

Let $p(b,d)$ be the conditional probability that an emission, occured in pixel b, is detected in tube d. Then $n^*(d)$, total number of emittions detected in tube d, has poisson distribution with mean $\lambda^*(d)=\sum_{b=1}^{B}\lambda(b)p(b,d)$. Here $p(b,d)$'s are assumed known nonnegative constants. It depends on various factors: the geometry of the detection system, the activity of the isotope and exposure time, and the extent of attenuation and scattering between source and detectors. Here we estimate $p(b,d)$ as the angle of view from the center of the pixel b into tube d. Log of likelihood function is as follow

$$\ln L(\lambda)=\sum_{d=1}^{D}\left\{-\sum_{b=1}^{B}\lambda(b)p(b,d)+n^*(d)\ln\left(\sum_{b=1}^{B}\lambda(b)p(b,d)\right)-n^*(d)!\right\}.$$

Applying EM algorithm, we have the following iterative formula(Vardi, Shepp and Kaufman, 1985)

$$\lambda^{new}(b)=\lambda^{old}(b)\sum_{d=1}^{D}\left(\frac{n^*(d)p(b,d)}{\sum_{b'}\lambda^{old}(b')p(b',d)}\right).$$

2.2 priors for the emission intensity

Images reconstructed by using EM algorithm have been observed to become noisy and to have checkerboard effects. Also, these have large distortion near edges as the algorithm converges to the MLE. Snyder and Miller(1985) use Grenader's method of sieves to stabilize the results. Levitan and Gabor(1987) use a Gaussian prior, called penalty function, to prevent the occurrence of checkerboard effects. Since the posterior is sensitive only to local properties of priors, we use Markov Random Field(MRF) as priors. Hammersly-Clifford theorem states that Gibbs distribution is MRF, which has following form

$$p(\vec{\lambda}) \propto \exp\Big(-\sum_{c\in C} V_c(\vec{\lambda})\Big),$$

where c is a clique and C is the collection of all cliques. A local set of point c is clique if (b, b') are neighbors for $\forall(b, b')\in c$. Green(1990) suggests $V_c(\vec{\lambda})$ as follow;

$$V_c(\vec{\lambda}) = \beta \sum_{(b,b')\in c} w_{bb'} \log\cosh\Big(\frac{\lambda(b)-\lambda(b')}{\delta}\Big),$$

where $w_{bb'}$ is a weight and $w_{bb'}=1$ if (b, b') are orthogonal neighbors, $\sqrt{1/2}$ if (b, b') are diagonal neighbors and 0 otherwise. Bouman and Sauer(1993) propose edge-preserving prior, called generalized Gaussian Markov random field, which allows realistic edge modeling having form

$$\ln p(\vec{\lambda}) = -\beta^k\Big(\sum_b a_b\lambda(b)^k + \sum_{c\in C}\sum_{\{b,b'\}\in c} w_{bb'}|\lambda(b)-\lambda(b')|^k\Big) + constant,$$

where $1\le k\le 2$. GGMRF includes Gaussian MRF when $k=2$ and is similar to median pixel prior suggested by Besag(1986) when $k=1$. It includes only pair interaction in the clique.

2.3 Bayesian EM(BEM)

With GGMRF prior, we have the posterior as follow

$$\ln p(\vec{\lambda}|\vec{n^*}) = \sum_{d=1}^{D} n^*(d)\ln\Big(\sum_b \lambda(b)p(b,d)\Big) - \sum_d\sum_b \lambda(b)p(b,d) - V(\vec{\lambda}) + constant$$

$$\text{where}\quad V(\vec{\lambda}) = \beta^k\Big(\sum_b a_s\lambda(b)^k + \sum_{c\in C}\sum_{\{b,b'\}\in c} w_{bb'}|\lambda(b)-\lambda(b')|^k\Big).$$

Let $z(b, d)$ be an estimate of unobserved data $n(b, d)$ given observed data $n^*(d)$. Then $z(b,d) = E(n(b,d)|n*(d)) = n^*(d)\dfrac{\lambda(b)p(b,d)}{\sum_{b'}\lambda(b')p(b',d)}$.

Using this result, we have the following result at the expectation step

$$E(\ln p(\vec{\lambda}|\vec{n}, \vec{n^*})|\vec{n^*}, \vec{\lambda}^{old}) = \sum_d \sum_b z(b,d) \ln \lambda(b) p(b,d) - \sum_d \sum_b \lambda(b) p(b,d) - V(\vec{\lambda}).$$

At the maximization step, find a estimate of $\vec{\lambda}$ which maximize above equation and go back to expectation step putting the estimate as $\vec{\lambda}^{old}$. Instead of direct maximization, we use one-step-late(OSL) approximation proposed by Green(1990). We have the following iterative equation

$$\lambda^{new}(b) = \frac{\sum_d z(b,d)}{\sum_d p(b,d) + \frac{\partial V(\vec{\lambda})}{\partial \lambda(b)} \mid_{\lambda = \lambda^{old}}}.$$

Green(1990) uses Bayesian reconstruction for PET and there are lack of clarity in the reconstructed image near edges.

3. Bayesian EM with line process(LBEM)

The objective of the line process is to detect the presence and identify the location of intensity changes in an image and then to eliminate the pixels having edge element from neighborhood. Let $l(b, b') = 1$ if there exists edge element between pixel b and b', 0 if not. We use hierachical model for the priors. Then edge-preserving priors with line process has the following form

$$p(\vec{\lambda}, \vec{l}) \propto \exp\{ - V_1(\vec{\lambda}|\vec{l}) - V_2(\vec{l}) \},$$

$$V_1(\vec{\lambda}|\vec{l}) = \beta^k \Big(\sum_b a_b \lambda(b)^k + \sum_{c \in C} \sum_{\{b,b'\} \in c} (1 - l(b,b')) w_{bb'} |\lambda(b) - \lambda(b')|^k \Big).$$

Geman and Geman(1984) use clique of size four to construct $V_2(\vec{l})$. Applying EM algorithm with the above prior and Poisson likelihood function, we have

$$\lambda^{new}(b) = \frac{\sum_d z(b,d)}{\sum_d p(b,d) + \frac{\partial V_1(\vec{\lambda}|\vec{l})}{\partial \lambda(b)} \mid_{\lambda = \lambda^{old}, \, l = l^{old}}},$$

$$l(b,b')^{new} = 1 \text{ or } 0 \text{ which minimize } \{ V_1(\vec{\lambda}|\vec{l}) + V_2(\vec{l}) \}|_{\lambda = \lambda^{old}, \, l = l^{old}}.$$

Here we determine $l(b, b')$ using empirical distribution of the difference of the pixel intensities of b and b'. Here is the procedure for the line process. We call it as empirical line process. First, we consider clique of size four and four types of pair interactions: horizonal, vertical, right-skewed diagonal and left-skewed diagonal. Let F_i be the empirical

distribution of $d_{ij}(b, b')$ with $(b, b') \in c$ where $d_{ij}(b, b')$ is the difference of the two pixel intensities of i type pair interaction, $i = 1, 2, 3, 4$ with $j = 1, 2, \cdots, N_i$, the number of two neighboring pixels. Second, determine the p_i which is the proportion of pixels having i type edge relations in the image. The p_i is determined by examining the empirical distribution of $d_{ij}(b, b')$. If there is the point from which the right side is flat, then p_i is the right-tail probability from this point. Third, find $(1-p_i)^{th}$ percentile point of F_i, $F_i^{-1}(1-p_i)$, and determine $l(b, b') = 1$ if $d_{ij}(b, b') \geq F_i^{-1}(1-p_i)$ and 0 otherwise. The LBEM algorithm is as follows.

Step 1: Apply BEM(Bayesian EM) to the data with initial estimate $\vec{\lambda}^{(0)}$.

Step 2: Applying the empirical line process to the result obtained after K iterations of BEM, determine $l(b, b')$.

Step 3: Calculate $\lambda^{new}(b)$ and go to Step 2 with the data $\lambda^{new}(b)$ until it satisfies the convergence criteria.

When this algorithm is applied to the result obtained after K iteration of EM, we call it LEM(EM with line process).

4. Simulations and Results

We study two-dimensional reconstruction. We assume a single ring of radius $\sqrt{2}$ with equally spaced detectors around the phantom with $B = 100 \times 100$. We use the phantom in Fig. 1(a), which is used to generate the data and which we want to reconstruct. The histogram of the 10^6 counts drawn from the phantom of Fig. 1(a) at a rate proportional to $\lambda(b, d)$ is in Fig. 1(d). We use uniform values as initial estimate of $\vec{\lambda}$. The images in Fig. 1(b), (c), (e) and (f) are the results of the EM, BEM, LEM and LBEM algorithm after 32 iterations respectively. The image with EM has checkerboard effects as expected. To apply BEM, we use $\beta = 0.01$, $k = 1.05$ and $a_b = 0$ for $b = 1, 2, \cdots, B$ as parameters for the prior. Checkerboard effects are suppressed in the image of BEM. The reconstructed images are settled down around 20 iterations according to our simulation. However, it shows the lack of clarity around edges. We adapt the empirical line process to the result of EM and BEM after 16 iterations respectively. We choose K=16. The result of LEM after 32 iteratons(including 16 iteration of EM) shows suppression of the noise and improvements around edges. Since empirical line process introduce a prior in the model, this algorithm has smoothing effects on the image except edges. The result of LBEM after 32 iteratons(including 16 iteration of BEM) shows improvement of the clarity around edges. The results of applying empirical line

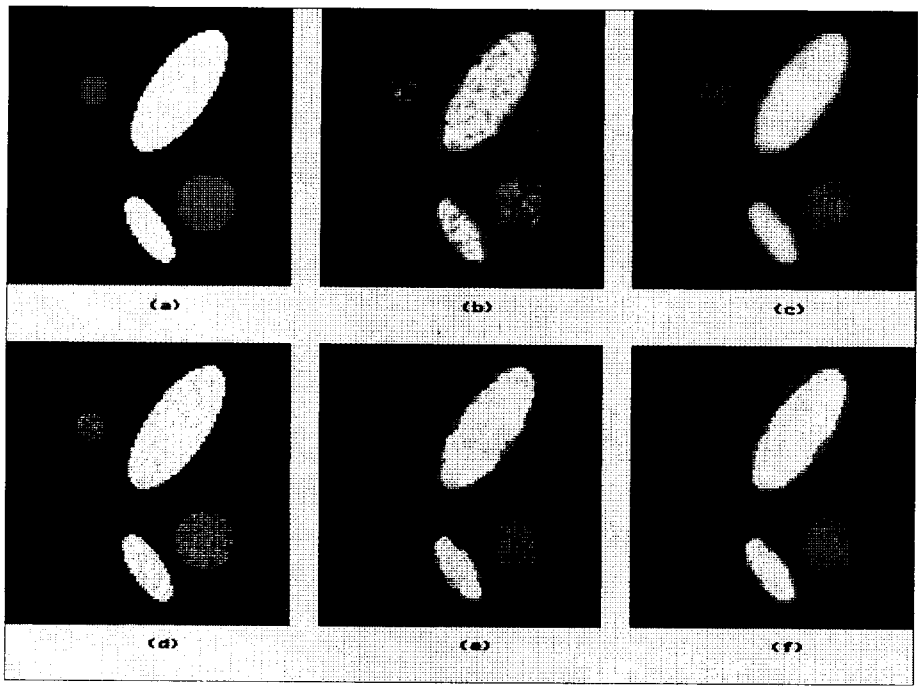

Fig. 1 (a) real image (b) EM after 32 iterations (c) BEM after 32 iterations (d) histogram of 10^6 emissions (e),(f) LEM and LBEM after 32 iterations resp.

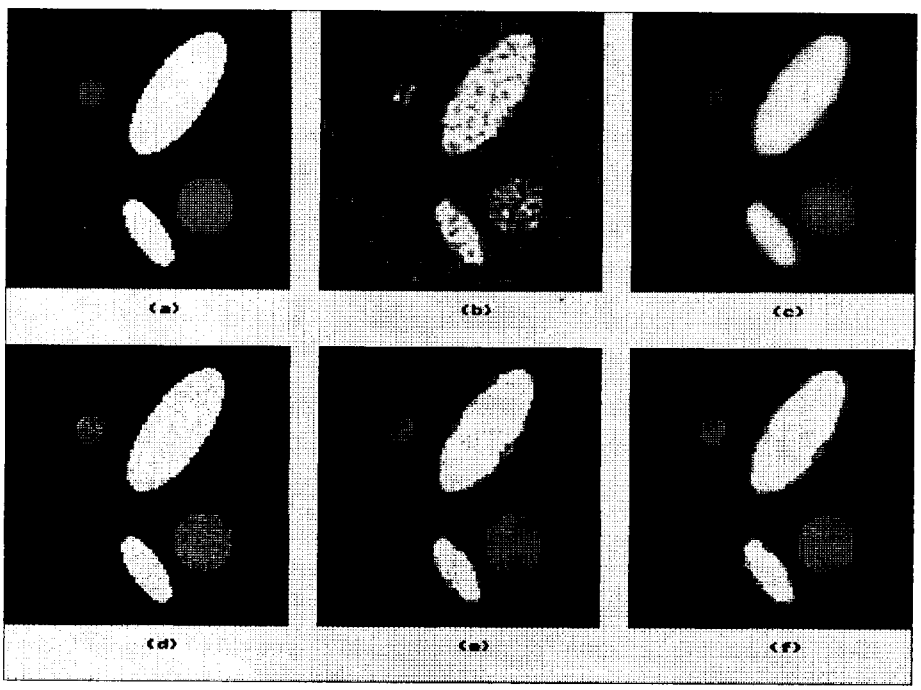

Fig. 2 (a) real image (b) EM after 64 iterations (c) BEM after 64 iterations (d) histogram of 10^6 emissions (e),(f) LEM and LBEM after 64 iterations resp.

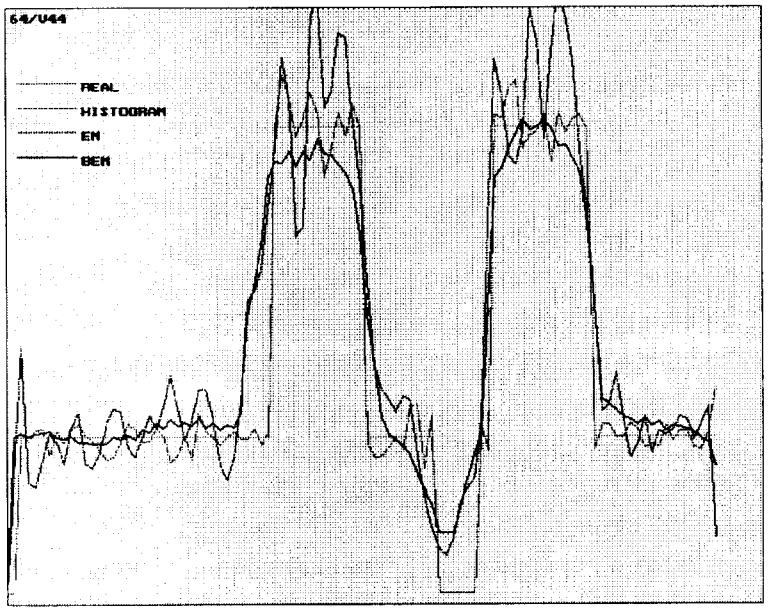

Fig. 3 Line plot of real, histogram, EM and BEM through 44th column.

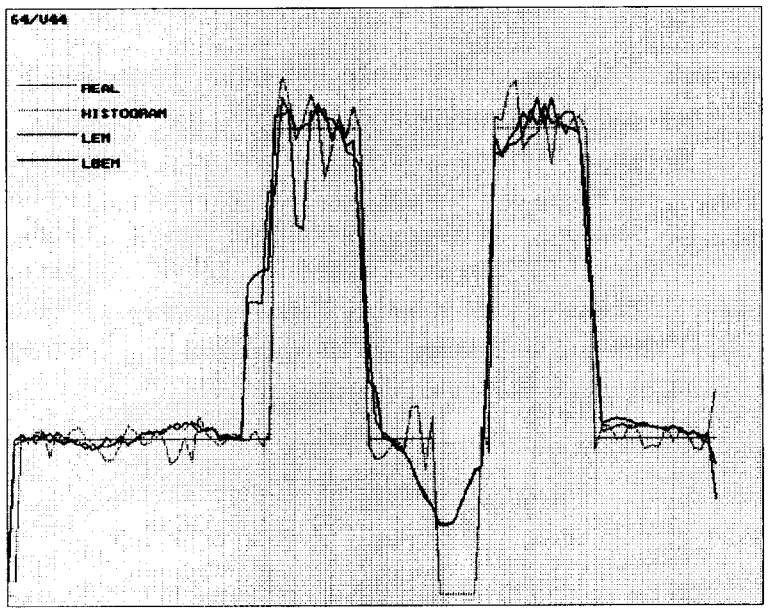

Fig. 4 Line plot of real, histogram, LEM and LBEM through the 44th column.

process (LEM and LBEM) show clear edge elements compare to the result of EM and of BEM. The differences between Fig.1(b)(c) and Fig. 1(e)(f) occur at the edge points. The results of 64 iteration are given in Fig. 2. Fig. 2(a)(d) are same as Fig 1.(a)(d). The images

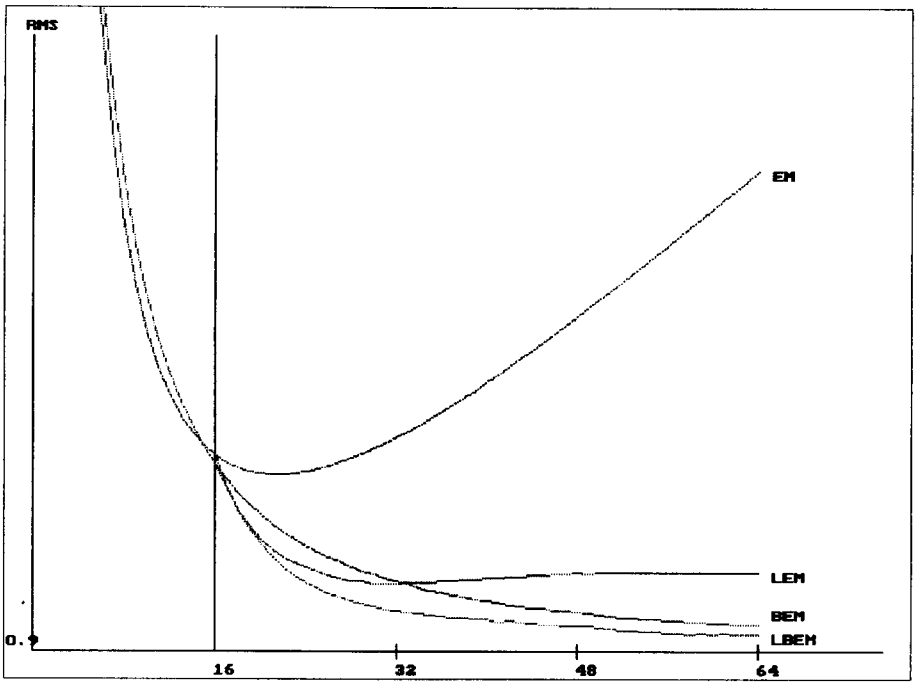

Fig. 5 Root mean square error of EM, BEM, LEM and LBEM

in Fig. 2(b), (c), (e) and (f) are the results of the EM, BEM, LEM and LBEM algorithm after 64 iterations respectively. The reconstructed image with EM tends to get worse as the iterations go on. The results of LEM and LBEM show the clear improvement in the noise and edges. To check the accuracy, we draw a line plot of the 44th column from the left of the images obtained after 64 iterations. In Fig. 3, line plot of real, histogram, EM and BEM are drawn. In Fig. 4, a line plot of real, histogram, LEM and LBEM are drawn. These show that EM has noise artifacts, BEM suppresses noise artifacts but has smoothing effect at the edges. LEM and LBEM detect edge elements correctly at the edges. We compare root mean square error(RMS) as an overall measure of reconstruction accuracy.

$$\mathrm{RMS} = \sqrt{\frac{\sum_{b=1}^{B}(\lambda(b)-\hat{\lambda}(b))^2}{B}} .$$

In Fig. 5, RMS of EM is increased as iterations go on. This indicates that reconstructed image is deteriorated by noise as iterations go on. Since BEM has smoothing effects, RMS is decreased. RMS of LEM and LBEM are decreased until 32 iterations and then those are stabilized as iterations proceed. Because of edge elements, there is not much changes in the reconstructed images.

5. Conclusions

In this paper we propose a line process for EM and BEM, we call LEM and LBEM respectively, for image reconstruction of PET. These algorithms suppress the checkerboard effects occuring in the EM algorithm and overcome the smoothing effects near edges occuring in the BEM. Based on RMS, reconstructed images using these algorithms have become stable as iterations proceed. Appropriate choice of priors is important since the results are sensitive to the priors.

References

[1] Besage, J.E. (1986). On the Statistical Analysis of Dirty Pictures, *Journal of Royal Statistical Society*, Ser. B, Vol. 48, No. 3, 259-302.

[2] Bouman, C., and Sauer, K. (1993). A Generalized Gaussian Image Model for Edge_Preserving MAP Estimation, *IEEE Transactions on Image Processing*, Vol. 2, No. 3, 296-310.

[3] Geman, S., and Geman, D. (1984). Stochastic Relaxation, Gibbs Distributions, and the Bayesian Restoration of Images, *IEEE Transactions on Pattern Analysis and Machine Intelligence*, Vol. PAMI-6, No. 6, 721-741.

[4] Green, P. J. (1990). Bayesian Reconstructions From Emission Tomography Data Using a Modified EM Algorithm, *IEEE Transactions on Medical Imaging*, vol. 9, No. 1, 84-93.

[5] Herman, G. T. (1980). *Image Reconstruction from Projection*, Academic Press.

[6] Levitan, E., and Herman, G. T. (1987). A Maximum A Posteriori Probability Expectation Maximization Algorithm for Image Reconstruction in Emission Tomography, *IEEE Transactions on Medical Imaging*, vol. MI-6, No. 3, 185-192.

[7] Snyder D.L., and Miller M. I. (1985). The Use of Sieves to Stabilize Images Producded with the EM Algorithm for Emission Tomography, *IEEE Transactions on Nuclear Science*, Vol. NS-32, No. 5, 3864-3872.

[8] Vardi, Y., Shepp, L A., and Kaufman, L. (1985). A Statistical Model for Positron Emission Tomography, *Journal of the American Statistical Association*, Vol. 80, 8-37.